

The rumble sound generated by a tidal bore event in the Baie du Mont Saint Michel

Hubert Chanson^{a)}

Department of Civil Engineering, The University of Queensland, Brisbane QLD 4072, Australia

(Received 24 November 2008; revised 27 March 2009; accepted 1 April 2009)

A tidal bore is a sharp rise in free-surface elevation propagating upstream in an estuarine system at the leading edge of the flood tide. It generates a powerful noise that was sometimes compared to the sounds of a horse cavalcade. Herein the sounds generated by a tidal bore event in the Baie du Mont Saint Michel were carefully recorded. The data showed three distinct periods. These were the incoming tidal bore when the sound amplitude increased with the approaching bore front, the passage of the tidal bore in front of the microphone where the impacts of the bore on the bank, rocks, or jetty generated powerful noises, and the upstream propagation of the bore when the flood flow motion caused additional loud noises. During the arrival of the tidal bore, the sound levels were less energetic and a lower-pitch sound was noted than during the subsequent record. For the breaking bore process, the analysis of the sound record indicated a dominant frequency around 76–77 Hz. The low-pitch rumble had a frequency comparable to the collective bubble oscillations, suggesting that air entrapment in the bore roller might play a major role in the acoustic signature. © 2009 Acoustical Society of America. [DOI: 10.1121/1.3124781]

PACS number(s): 43.28.Ra, 43.28.Tc, 43.30.Nb, 43.30.Pc [KVH]

Pages: 3561–3568

I. INTRODUCTION

A tidal bore is a sharp rise in free-surface elevation propagating upstream in an estuarine system as the tidal flow turns to rising. Also known as aegir, mascaret, or pororoca, a tidal bore forms typically during spring tide conditions with tidal ranges exceeding 4–6 m when the flood tide converges into a narrow funneled channel. Figure 1 illustrates a tidal bore event in the Baie du Mont Saint Michel (France), while Fig. 2(a) shows the promontory from where the photographs were taken. Figure 2(b) presents a map of the area.

A tidal bore creates a powerful sound. In China, the noise of the Qiantang River bore was compared to “the clamor of a hundred thousand troops” in a poem by Guo of the Tang dynasty and to “10 000 horses break out of an encirclement (Chen *et al.*, 1990), crushing the heavenly drum, while 56 huge legendary turtles turn over, collapsing a snow mountain” by the Chinese poet Yuan during the Yuan dynasty (Dai and Zhou, 1987). The sounds generated by a tidal bore were also called a “roar” (Darwin, 1897) or a “great destructive noise” and compared to the sound of locomotive train, of bass drums, of thunder, and of torrential flows. A Canadian composer, Monahan, created a musical piece that was a metaphorical interpretation of the tidal bore action, using sound recordings of water flow from the Bay of Fundy: “the tidal bore of the Maccan River” (Monahan, 1981).

The noise generated by a tidal bore combines sounds caused by the turbulence in the bore front and whelps, entrained air bubbles in the bore roller (“white waters”), sediment erosion beneath the bore front and of the banks, scouring of the sandbars, and impacts on obstacles (rocks and bridge piers). The bore rumble can be heard far away be-

cause low frequencies can travel over long distances. During his expedition in the Qiantang River mouth, Moore almost lost his survey ship and two steam cutters on 20 September 1888 when he inadvertently anchored in the Qiantang River estuary; he heard the first murmur of the bore 1 h before it reached his Pandora ship (Moore, 1888, p. 7). In the Baie du Mont Saint Michel, the writer heard often the tidal bore 25–30 min before the bore front reached him. Animals can be more sensitive to the tidal bore sounds than the human ear (Warfield, 1973; Fay, 1988; *Encyclopædia Britannica*, 2008). When the bore closes in, the rumbling noise disorients some species. In the Baie du Mont Saint Michel, sheep have been outrun and drowned by the tidal bore. In Alaska, moose have tried unsuccessfully to outrun the bore (Molchan-Douthit, 1998). In each case, the animals were panicked with the deafening noise of the bore although they could run faster than the bore front.

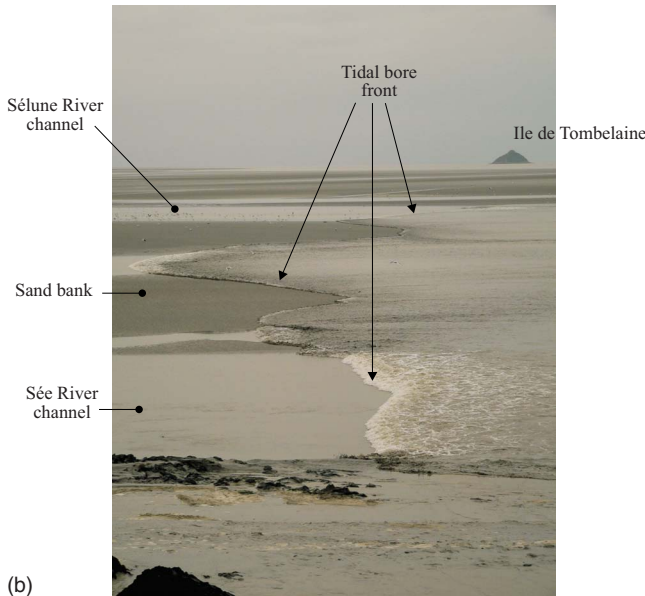
A tidal bore is somehow a continuous breaking “wave,” and passive acoustic techniques were used successfully to characterize to wind-generated wave breaking and the entrained air bubbles (Loewen and Melville, 1991; Manasseh *et al.*, 2006). The air bubble entrainment process is indeed fundamental to the air-sea interactions (Melville and Rapp, 1985; Wallace and Wirick, 1992; Chanson and Cummings, 1994). Most studies of wave breaking used underwater hydrophones (Felizardo and Melville, 1995; Manasseh *et al.*, 2006). Some investigated similar flow patterns to study specific features of the entire process (e.g., Nicholas *et al.*, 1993; Kolaini *et al.*, 1994). Passive acoustic techniques were also used successfully to investigate sediment transport under waves and in tidal flows (Thorne, 1986; Mason *et al.*, 2007).

Although there are numerous anecdotal observations, the acoustic properties of a tidal bore have not been investigated in detail until now. Herein, the atmospheric sounds of a tidal bore event were carefully recorded, and the passive acoustic

^{a)}Electronic mail: h.chanson@uq.edu.au



(a)



(b)

FIG. 1. (Color online) Tidal bores in the Baie du Mont Saint Michel (France) on 14 October 2008 evening. (a) Breaking bore of the Sée-Sélune River system North of Pointe du Grouin du Sud on 14 October 2008 evening. The photograph was taken shortly before the tidal bore divided into the Sée and Sélune River channels, with Bec d'Andaine in the upper left of the photograph. (b) Tidal bore of the Sée and Sélune Rivers at Pointe du Grouin du Sud on 14 October 2008 evening. Note the Sée River bore in the foreground with the rocky promontory of Pointe du Grouin du Sud (bottom left) and the Sélune River bore in the background with Ile de Tombelaine (top right).

characteristics were analyzed. The present work takes preliminary steps toward an acoustic signature technique for characterizing a tidal bore process.

II. STUDY SITE AND FIELD MEASUREMENTS

The Baie du Mont-Saint-Michel (France) in the English Channel (La Manche) is characterized a very large tidal range (up to 14 m) and fast advancing flood tides. The Baie is drained by three main rivers: the Couesnon, the Sélune, and the Sée [Fig. 2(b)]. In the past, the hydrodynamics and sedimentology of the Baie, including the access to the Mont Saint Michel, were mostly affected by the strong flows of the Couesnon and Sélune Rivers. The Sélune River is 70 km

long with a catchment area of 1010 km², and it constitutes the most significant freshwater inflow into the Baie du Mont Saint Michel. At its mouth between Roche-Torin and Pointe du Grouin du Sud, the Sélune River joins the Sée River, and the waters merge at low tides.

During spring tides, the Baie du Mont Michel is subjected to several tidal bore processes. Larsonneur (1989) mentioned briefly a tidal bore near Pointe du Grouin du Sud propagating at about 2.5 m/s. Tessier and Terwindt (1994) discussed the effect of tidal bore on sediment transport downstream of the Sée and Sélune river mouths. Chanson (2005a, 2005b, 2008a) presented photographic evidences of the tidal bore processes and discussed their impact on the Baie.

Herein the tidal bore of the Sée-Sélune River system was observed at the Pointe du Grouin du Sud in the Baie du Mont Saint Michel on the 14 October 2008 early evening when photographs and video movies were taken (Fig. 1), and again at the next flood tide on 15 October 2008 early morning. It was a full moon and the tidal range was 12.55 m. During the latter event, the sounds were recorded with a digital video camcorder Canon MV500i equipped with a stereo electret condenser microphone. The microphone was fixed to the camera and its signal-to-noise ratio (SNR) setting is fixed for the duration of each recording. The audio signal pulse-code modulation (PCM digital sound: 16 bit, 48 kHz/2 channels) was separated from the video signal, and the WAV file is available in a digital appendix. Note that the audio recording was taken by the author alone. The closest livestock was 500 m away, and the nearest dwelling 1 km away.

The video camera and microphone were placed on the rocky promontory (Fig. 2). Its location was fixed (about 45–50 m from the western edge of the rocky promontory) but the microphone was moved to follow the tidal bore front for the whole duration of the record. Figure 2(a) indicates the exact location of the camcorder. A miniDV tape recorder digitized the signal at 32 kHz, implying a Nyquist frequency of about 16 kHz. The range of tidal bore conditions caused a difference in acoustic signal power of up to 20 dB corresponding to a factor of 10 in sound amplitude during the record. Since all data recorded on tape should have similar magnitudes to minimize distortion or loss of dynamic range, the entire record was sub-divided into three periods of comparable sound amplitude to deliver comparable recorded quality during the signal processing. The WAV recordings were processed with the software DPLOT™, Version 2.2.1.6. Fast Fourier transforms were taken. Each experimental data set was sub-sampled into sub-sets 2 s long to give a frequency span of 0–16 kHz.

Further details on the field study were reported by Chanson (2008a).

III. FIELD OBSERVATIONS

A. Presentation

On 15 October 2008, the tidal bore (*mascaret*) was seen in the morning darkness about 1 h before sunrise. The sky was cloudy and there were intermittent showers. The tidal bore arrived from the Sée-Sélune River channel [Figs. 1(a)

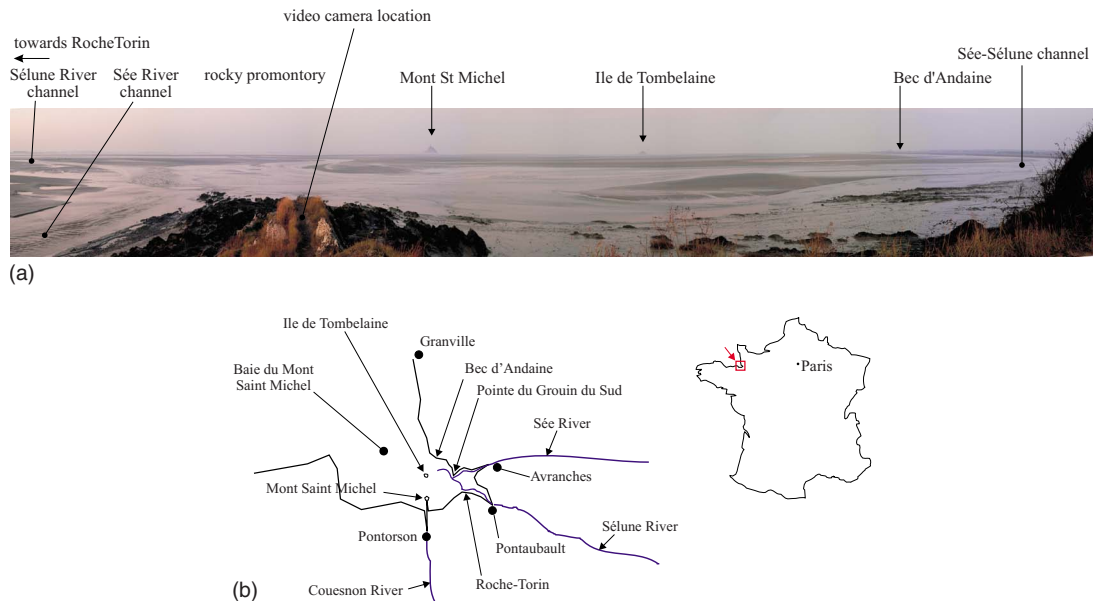


FIG. 2. (Color online) Photograph and sketch of the Baie du Mont Saint Michel (France). (a) Panoramic view of the Baie du Mont Saint Michel seen from the Pointe du Grouin du Sud on 19 October 2008 at 08:20 at sunrise and low tide. Note the rocky promontory of Pointe du Grouin du Sud in the foreground, the Mont Saint Michel and Ile de Tombelaine in the background, and the joint Sée-Sélune River system on the right of the photograph. (b) Sketch of the Baie du Mont Saint Michel and the Sée and Sélune Rivers.

and 2(a) right]. The bore front passed the rocky promontory of the Pointe du Grouin du Sud at 06:50. It entered into the Sée River channel while another tidal bore continued into the Sélune River channel toward Roche-Torin and Pontaubault [Fig. 2(a) left]. The entire process was a breaking bore, similar to the one photographed 12 h earlier (Fig. 1). In the darkness, the white waters of the breaking bore were clearly seen with a torch, but there was not enough light for photographic observations.

The sound measurements started at 06:48 and lasted for about 4 min (Fig. 3). The entire bore sound record may be sub-divided into three consecutive periods. From the first 95 s of the record, the tidal bore approached Roche-Torin and the sound amplitude gradually increased. For $95 < t < 130$ s, the tidal bore reached the rocky promontory seen in Figs. 1(b) and 2(a) and “crashed” onto the rocks, yielding loud and powerful noises. The tidal bore was just in front of the promontory in the same position as in Fig. 1(b) for $t = 100–102$ s (visual observation with a torch at 06:50). For $130 < t < 221$ s, the tidal bore continued into the Sée River channel toward Avranches and in the Sélune River channel toward Roche-Torin and Pontaubault. During this third period, the audio record was a combination of the sounds generated by the tidal bore in the Sée River channel that was in the foreground, the flood tidal flow past the rocky promontory of Pointe du Grouin du Sud, and the tidal bore in the Sélune River channel in the background (Fig. 2).

The entire sound record is presented in Fig. 3, and the three distinct periods are highlighted.

The acoustic properties of the record were analyzed in terms of the absolute value of the sound pressure amplitude. Typical results are summarized in Table I (columns 5 and 6), showing the mean and standard deviation of the amplitude modulus. It is seen that the noises during the second period, when the tidal bore passed around the rocky promontory, were in average five times louder than during the first period (incoming bore). The quantitative data were supported by the personal observations during the event. The ratio of standard deviation to mean absolute value was typically between 1.1 and 1.5 for the complete study, nearly independent of the period.

A spectral analysis was conducted, and the basic properties are summarized in Table I (columns 7 and 8). The acoustic spectra are shown in Fig. 4 for each period of the sound record presented in Fig. 3. Each spectrum exhibited a minimum in energy below 5 Hz, indicating that the low-frequency rumbling noise of the tidal bore noise was above 5 Hz, within the entire audible range of sounds for a human ear (Encyclopædia Britannica, 2008). In each spectrum, a dominant frequency was observed, and the characteristic values are summarized in Table I (column 7). The dominant frequency ranged from 74 to 131 Hz depending on the period,

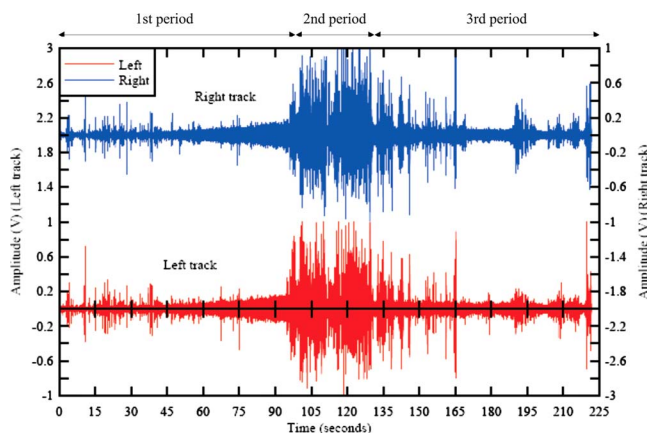


FIG. 3. (Color online) Audio signals of the tidal bore of the Sée-Sélune River at Pointe du Grouin du Sud on 15 October 2008 between 06:48 and 06:52.

TABLE I. Acoustic properties of tidal bore sound record.

| Reference | Record | Duration (s) | Audio track | Average sound amplitude modulus (V) | STD sound amplitude modulus (V) | Dominant frequency (Hz) | Integral of PSD function 0–16 kHz (V ²) | Remarks |
|---|-----------------------|---------------|-------------|-------------------------------------|---------------------------------|-------------------------|---|--|
| Sée-Sélune River tidal bore, 15 Oct. 2008 | Tidal bore (breaking) | First period | Left | 0.0159 | 0.0178 | 76.2 | 1.234 | From Pointe du Grouin du Sud (right bank) Incoming tidal bore |
| | | | Right | 0.0143 | 0.0160 | 76.7 | 1.181 | |
| | Second period | Left | 0.0786 | 0.0851 | 130.9 | 3.625 | | |
| | | Right | 0.0840 | 0.0920 | 113.3 | 3.858 | | |
| | Third period | Left | 0.0230 | 0.0326 | 92.3 | 1.356 | Bore, whelps, and flood flow | |
| | | Right | 0.0249 | 0.0379 | 73.8 | 1.501 | | |
| Sée-Sélune River, 15 Oct. 2008 | Whelps | Entire record | Left | 0.0455 | 0.0502 | 125.4 | 1.663 | From Pointe du Grouin du Sud (right bank), 3–5 min after bore passage |
| | | | Right | 0.0414 | 0.0392 | 89.4 | 1.485 | |
| Dordogne River, 18 Oct. 2005 | Tidal bore (undular) | First period | Left | 0.0328 | 0.0275 | 191.4 | 1.611 | From Port de Saint Pardon (left bank) Incoming tidal bore |
| | | | Right | 0.0141 | 0.0113 | 233.4 | 0.800 | |
| | Second period | Left | 0.0988 | 0.0789 | 246.6 | 6.186 | Bore passage in front of jetty | |
| | | Right | 0.0676 | 0.0624 | 238.8 | 4.872 | | |

Note that Dordogne River data set was provided by Patrick Vialle, modulus is the absolute value, PSD is the power spectral density, and STD is the standard deviation.

and these values corresponded to a low-pitch sound, or rumble. Such a rumble frequency could be explicable by collective oscillations of bubble clouds entrapped in the bore roller and during wave breaking on the banks (Prosperetti, 1988; Kolaini *et al.*, 1994).

During the first period of the record, the tidal bore was a breaking bore advancing in the main channel and over sand banks and mudflats (Fig. 1). The low-frequency sound (76–77 Hz) may be considered to be a characteristic feature of the advancing roller, caused by the turbulence and entrained bubbles in the roller, sediment erosion beneath the advancing bore, and the scouring of channel edges, sand flats, sandbars, and shoals [Fig. 1(b)]. For the second period, the tidal bore impacted onto the rocky promontory, and the impact was an energetic process generating louder noises of

a higher pitch, yielding a dominant frequency around 113–131 Hz. This is clearly seen in Fig. 4 where the higher acoustic energy illustrates a louder noise, as well as by the integral of the power spectral density function (Table I, column 8). During the third period, the sounds were a combination of the tidal bores leaving the Pointe du Grouin du Sud in the Sée and Sélune River channels, as well as the impact of the flood flow on the promontory rocks. This yielded a slightly flatter, broader acoustic spectrum (Fig. 4). Note that, since all peak frequencies were greater than the low-frequency noise found below 5 Hz, no high-pass filtering was required.

B. Comparison with other tidal flows

The acoustic signature of the tidal bore event was compared with two other relevant sound records (Table I). One was the sound of the tidal bore whelps and flood flow measured at the Pointe du Grouin du Sud on 15 October 2008 between 06:54 and 06:56, about 4–5 min after the tidal bore passage at Pointe du Grouin du Sud. The data were recorded with the same microphone and at the same location as the tidal bore event, but the microphone was facing the Pointe du Grouin du Sud promontory for the entire recording. During this record, the sounds were a combination of the noises of the flood flow crashing on the rocks of the promontory, of the flood flow in the Sée River channel just below the Pointe du Grouin du Sud, and, in the far background, of the tidal bores in the Sée and Sélune River channels. The recorded sounds were powerful and quite violent.

The second record was taken from the left bank of the Dordogne River at Port de Saint Pardon on the 18 October 2005 during the passage of an undular tidal bore (Fig. 5). Figure 5 shows a photograph of the undular tidal bore of the Dordogne River at Port de Saint Pardon, but taken at a later

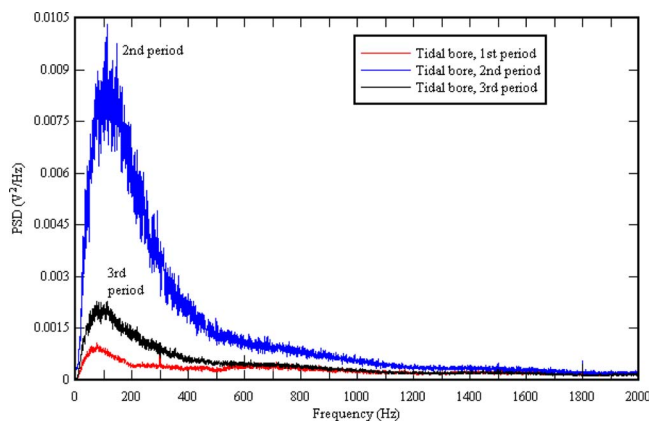


FIG. 4. (Color online) Acoustic spectra of the tidal bore event, Sée-Sélune River at Pointe du Grouin du Sud, Baie du Mont Saint Michel on 15 October 2008 between 06:48 and 06:52. Average of left and right sound track spectra.



FIG. 5. (Color online) Undular tidal bore of the Dordogne River at Port de Saint Pardon on 22 July 2008 evening. Note the first wave crest breaking on the jetty in the foreground and the surfer riding on the third wave.

date. The microphone was located in the vicinity of the jetty. It pointed toward the river channel and was fixed for the duration of the record. That data set is presented in Fig. 6. It shows a first period of the record corresponding to the arrival of the tidal bore toward Port de Saint Pardon while the second part was dominated by the successive breaking of the undulations on the jetty during and after the bore passage. See the breaking of the Dordogne River tidal bore undulations on the jetty in Fig. 5 (foreground left). In Fig. 6, note the difference between the left and right sound tracks that resulted from the stationary position of the microphone on the left bank.

The characteristics of these two records are reported in Table I and compared with the tidal bore sound record in the Baie du Mont Saint Michel on 15 October 2008.

The acoustic spectrum of the whelps and flood flow at Pointe du Grouin du Sud is presented in Fig. 7 where it is compared with the tidal bore event data set. The comparison is relevant since all the sound data were recorded with the same microphone from the same location. In Fig. 7, both horizontal and vertical axes have a logarithmic scale. The plots illustrate the minimum in energy at roughly 1–5 Hz for all data, as well as maxima for frequencies between 76 and 131 Hz. While all data sets corresponded to low-frequency noises, the loudness of the tidal bore impact on the rocky

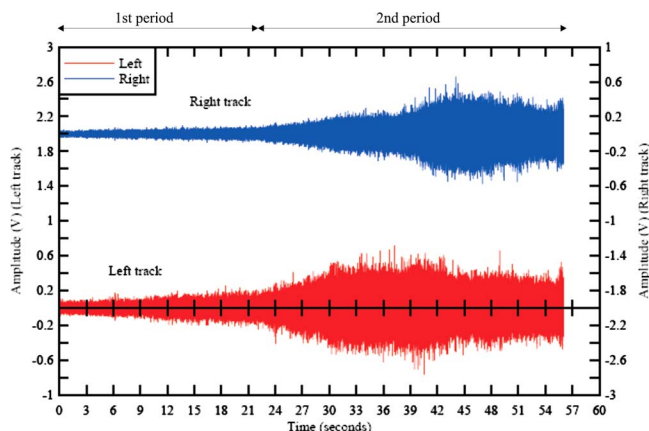


FIG. 6. (Color online) Audio signals of the tidal bore of the Dordogne River at Port de Saint Pardon on 18 October 2005.

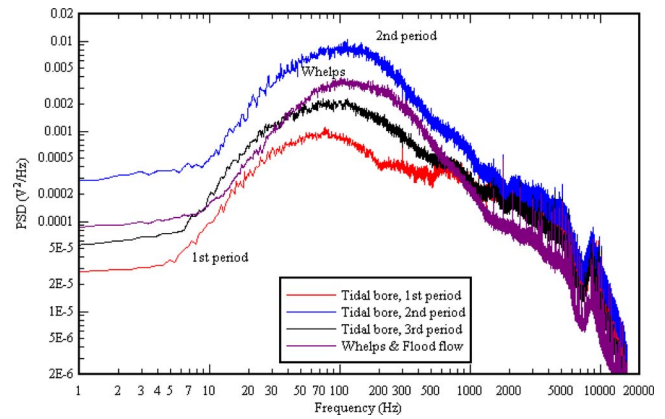


FIG. 7. (Color online) Comparison in acoustic spectra between the tidal bore (06:48–06:52), and its whelps and flood flow (06:53–06:55), at Pointe du Grouin du Sud, Baie du Mont Saint Michel on 15 October 2008. Average of left and right sound track spectra.

promontory of Pointe du Grouin du Sud is highlighted by its high acoustic energy (Fig. 7, tidal bore second period), and the second loudest sound record was that of the whelps and flood flow (Fig. 7).

The Dordogne and Sée-Sélune River tidal bores exhibited similar acoustic features during the first period of each record (Figs. 3 and 6). That is, an increasing sound level with increasing time, as well as a sound amplitude that was much lower than during the subsequent record sections. The acoustic spectra of the Sée-Sélune River and Dordogne River tidal bores showed some low-pitch sound frequency, with the Dordogne River tidal bore having a slightly higher dominant frequency (191–233 Hz) than that of the Sée-Sélune River tidal bore (Table I, column 7).

There were, however, some key differences between the two tidal bore events. First the Sée-Sélune River tidal bore was a breaking bore with a well-defined roller, while the Dordogne River tidal bore was an undular bore. It is believed that the turbulence and air bubble entrainment in the breaking bore roller in the Baie du Mont Saint Michel generated lower-frequency rumble sounds. Second, the Dordogne River tidal bore sound data were recorded with a fixed microphone, and there were a few background noises including voices. (The microphone was within 50 m from dwellings.) A limitation of the present analysis was indeed the quality in surrounding sounds. Because the sound amplitude falls off as $1/r$, and the sound power as $1/r^2$, where r is the radial distance to the microphone, sounds generated in the vicinity of the recording device contribute most to the measured sound. For example, people on the bank next to the microphone. On 15 October 2008, the sound recording in the Baie du Mont Saint Michel was conducted in the early morning in absence of spectators. This feature ensured a minimum level of background noise and a better characterization of the tidal bore acoustic signature, as shown by a comparison with the audio recording of the tidal bore at the same location on 14 October 2008 evening [Fig. 8(a)]. Figure 8 presents a comparison of the audio records of the same tidal bore recorded with the same equipment from the same location: (a) on the evening of the 14 October when the camcorder was surrounded by

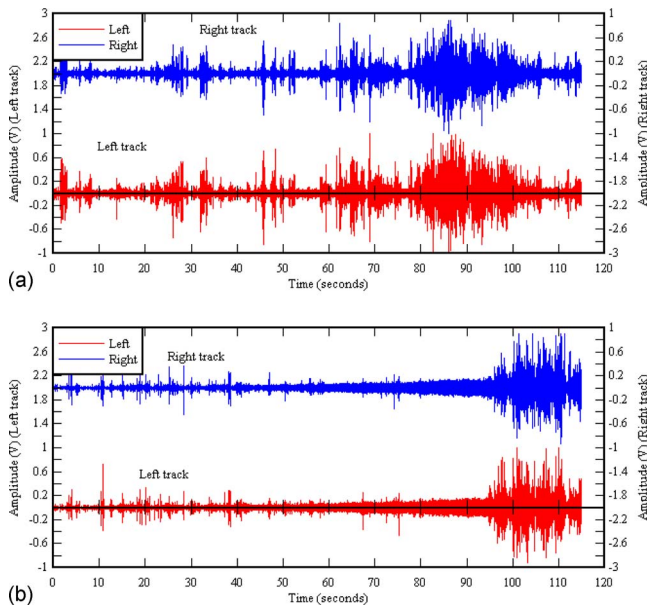


FIG. 8. (Color online) Audio signals of the tidal bore of the Sée River at Pointe du Grouin du Sud, Baie du Mont Saint Michel (France) during two successive tidal bore events. (a) On 14 October 2008 between 18:26 and 18:28. Tidal bore front passage at Pointe du Grouin du Sud: $t \sim 90$ s. (b) On 15 October 2008 between 06:48 and 06:52. Tidal bore front passage at Pointe du Grouin du Sud: $t \sim 100$ s.

several adults and children [Fig. 8(a)] and (b) on the early morning of 15 October when the closest livestock was 500 m away and the closest dwelling nearly 1 km away [Fig. 8(b)].

IV. DISCUSSION

In a breaking bore, large-scale vortical structures are generated at the roller toe and advected downstream (Hornung *et al.*, 1995; Koch and Chanson, 2009). The growth, advection, and pairing of these vortices are responsible for low-frequency oscillations of the turbulent velocity field in the bore roller. For example, some laboratory data yielded pulsation frequency F data corresponding to a Strouhal number $F \times d / V = 0.02$, where d is the initial water depth and V is the relative bore velocity, as seen a fluid particle traveling with the initial flow velocity (Chanson, 2008b). (Note that the findings are close for traveling bores and steady hydraulic jumps.) The bore roller is also characterized by some air bubble entrainment at the toe and advection in the roller (Fig. 9). Figure 9 illustrates the air bubble entrainment in the roller toe of an advancing breaking bore in laboratory. Using upon a conceptual model of a spilling breaker, Prosperetti (1988) showed that bubble generation at the roller toe can amplify the pressure oscillations induced by the large-scale turbulence. In a bubble cloud, the lowest natural frequency of the bubbly cloud is in first approximation

$$f_{\text{cloud}} = \frac{1}{L} \sqrt{\frac{P}{\rho \alpha}}, \quad (1)$$

where L is the bubble cloud characteristic length, P is the ambient pressure, ρ is the fluid density, and α is the void fraction (Prosperetti, 1988). The natural frequency of a bubble cloud is inversely proportional to $\alpha^{1/2}$ and to the cloud characteristic size. In a tidal bore, the bubbles are en-

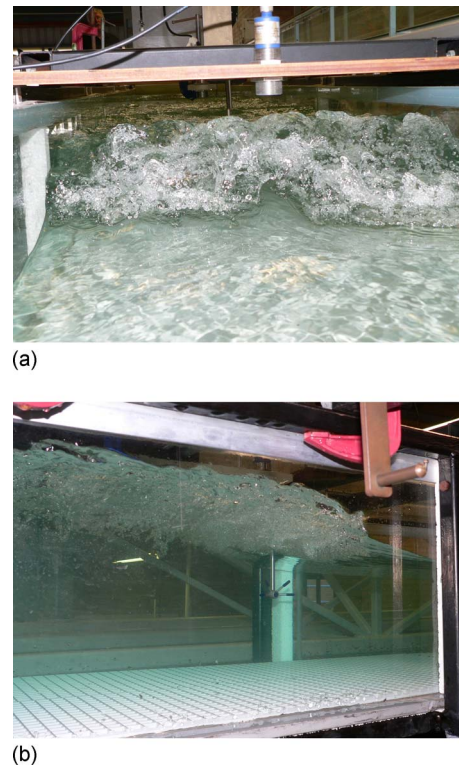


FIG. 9. (Color online) Photographs of breaking bore roller (shutter speed: 1/80 s). Laboratory data: $d = 0.14$ m, $Fr = 1.5$. (a) Looking at incoming bore roller. (b) Underside of the bore roller showing the entrained air bubble-bore propagation from left to right.

trapped in large-scale vortical structure and a characteristic dimension is the roller height (Fig. 9). Equation (1) would imply that large tidal bores would generate lower-pitch sound than small ones. Considering a bore height between 0.7 and 1 m as seen in Fig. 1, the lowest natural frequency of the bubbly cloud would be about 30–140 Hz for void fractions between 1% and 10%. For comparison, the field measurements by Kolaini *et al.* (1994) showed collective oscillations of bubble clouds within 44–190 Hz (Table II). The result tends to suggest that the air bubbles entrapped in the large-scale eddies of the tidal bore roller might be acoustically active and play a dominant role in the rumble sound generation.

In tidal channels and under waves, sediment motion by bed load and saltation induced particle collisions that transmit an acoustic pulse to the water. The acoustic signature of sediment transport was previously studied, and experimental results showed that the sounds have a high pitch with characteristic frequencies between 1.5 and 400 kHz (Thorne 1986; Mason *et al.*, 2007). That is, sediment motion was unlikely to be the dominant cause of the tidal bore rumble noise, but it might explain the secondary peak about 8–10 kHz in Fig. 7.

Table II presents a comparative summary of the dominant frequencies of the low-pitch rumble of tidal bores and of other processes, including bubble clouds, sediment bed load motion, breaking waves, and music instruments. The comparison shows, for example, that the sounds generated by the breaking bore had a low-pitch comparable to the sound generated by collective oscillations of rising bubble

TABLE II. Comparison of dominant sound frequencies generated by tidal bores and other processes.

| Type | Sub-type | Dominant frequency(ies) (Hz) | Remarks |
|---|-----------------------------|---------------------------------|--|
| Atmospheric observations | | | |
| Approaching tidal bores (First period) | Breaking bore | 76–77 | Sée River tidal bore, 15 Oct. 2008 |
| | Undular bore | 191–233 | Dordogne River, 18 Oct. 2005 |
| Locomotive train | 3000 Hp diesel locomotive | 60 | Measured at the engineer’s ear in the cabin (Maguire 2004) |
| | Locomotive whistle | ~400 | |
| Drums | Concert bass | 40–100 | |
| | Kettle | 8–150 | |
| Piano | A0 | 27.5 | Fundamental frequency |
| | A1 | 55 | |
| | Middle C | 246 | |
| | A4 | 440 | |
| Underwater observations | | | |
| Unsteady plunging jet | Field/laboratory data | 44–190 | Kolaini <i>et al.</i> (1994) |
| Rising bubble clouds | Laboratory data | 200–700 | Nicholas <i>et al.</i> (1993) |
| Steady plunging jet | Laboratory data | 1 200–4 000 | Chanson and Manasseh (2003) |
| Wave breaking | Laboratory data | 2 200–4 500 | Loewen and Melville (1991) |
| Gravel transport under waves | Large-scale laboratory data | 1 500–4 000 | Mason <i>et al.</i> (2007); $d_{50}=21$ mm |
| Rain drops | | 8 000–14 000 | Oguz and Prosperetti (1991) |
| Sediment bed load and saltation | Laboratory and field data | 20 000–400 000 | Thorne (1986); $d_{50}=25$ mm down to 0.3 mm |

clouds, bass drums, and trains. The latter may explain the “common analogy” between the sounds of breaking bores in the Qiantang River and Baie du Mont Saint Michel, and locomotive trains.

V. CONCLUSION

The sounds generated by a tidal bore event in the Baie du Mont Saint Michel were carefully measured. The sound record showed three distinct periods, and a similar feature was noted during another tidal bore event in the Dordogne River. These were (a) the incoming tidal bore when the sound amplitude increased with the approaching bore front, (b) the passage of the tidal bore in front of the microphone where the impacts of the bore on the bank, rocks, or jetty generated powerful noises, and (c) the upstream propagation of the bore when the whelps and flood flow motion caused additional loud noises. The distinction between periods was easily heard on site. Further the data highlighted the loudness of the noises generated during the whelps and flood flow several minutes after the tidal bore passage.

During the first period, the sounds generated by the incoming tidal bore were dominated by the bore front hydrodynamic processes including turbulence, air entrainment, breaking next to the banks, and sediment scour. A comparison between two tidal bore events illustrated both common features and differences. In each case, the approaching tidal bore generated an increasing sound with increasing time, and the sound levels were considerably lower than during the subsequent record sections. Both tidal events generated low-pitch sounds. For a breaking bore process, the audio record gave a lower-pitch sound (76–77 Hz) than during the undular bore event (191–233 Hz). It is likely that the difference in dominant sound frequencies resulted from some fundamental hydrodynamic differences between breaking and undular

tidal bores (Chanson, 2008b; Koch and Chanson, 2009). The low-pitch rumble of the breaking bore had a dominant frequency comparable to the collective oscillations of bubble clouds [Eq. (1)], suggesting that air entrapment in the bore roller is likely to play a major role in the acoustic signature of the bore.

In the future, however, the surrounding sound conditions should be carefully monitored, as well as the location of the microphone relative to the channel edge.

ACKNOWLEDGMENTS

The author acknowledges the helpful comments of Dr. Eric Jones, Dr. Pierre Lubin, and Dr. Richard Manasseh, of the reviewers, and of the associate editor. He thanks the people who provided him with valuable information, including (in alphabetical order) Jean-Yves Coccagn, Nathanaëlle Eudes, and Patrick Vialle. He further acknowledges the help of Ya-Hui Chou, Bernard Chanson, Nicole Chanson, and André Chanson during the field observations.

NOMENCLATURE

- d = initial water depth (m)
- d_{50} = median sediment size (m)
- Fr = surge Froude number
- F = turbulence frequency (Hz)
- f = sound frequency (Hz)
- L = bubble cloud characteristic length
- P = pressure
- r = distance (m) to the microphone
- t = time (s)
- α = void fraction
- ρ = water density (kg/m^3)

- Chanson, H. (2005a). "Mascaret, aegir, pororoça, tidal bore. Quid? Where? When? How? Why?," *Jl La Houille Blanche*, **3**, pp. 103–114.
- Chanson, H. (2005b). "Tidal bore processes in the Baie du Mont Saint Michel (France): Field observations and discussion," Proceedings of the 31st Biennial IAHR Congress, Seoul, Korea, edited by B. H. Jun, S. I. Lee, I. W. Seo, and G. W. Choi, Theme E.4, Paper No. 0062, pp. 4037–4046.
- Chanson, H. (2008a). "Photographic observations of tidal bores (mascarets) in France," Hydraulic Model Report No. CH71/08, The University of Queensland, Brisbane, Australia.
- Chanson, H. (2008b). "Turbulence in positive surges and tidal bores. Effects of bed roughness and adverse bed slopes," Hydraulic Model Report No. CH68/08, The University of Queensland, Brisbane, Australia.
- Chanson, H., and Cummings, P. D. (1994). "Effects of plunging breakers on the gas contents in the oceans," *Mar. Technol. Soc. J.* **28**, 22–32.
- Chanson, H., and Manasseh, R. (2003). "Air entrainment processes in a circular plunging jet. Void fraction and acoustic measurements," *ASME Trans. J. Fluids Eng.* **125**, 910–921.
- Chen, J. Y., Liu, C. Z., Zheng, C. L., and Walker, H. J. (1990). "Geomorphological development and sedimentation in Qiantang Estuary and Hangzhou Bay," *J. Coastal Res.* **6**, 559–572.
- Dai, Z., and Zhou, C. (1987). "The Qiantang bore," *Int. J. Sediment Res.* **1**, 21–26.
- Darwin, G. H. (1897). "The tides and kindred phenomena in the solar system," *Lectures Delivered at the Lowell Institute, Boston* (Freeman, London, 1962).
- Encyclopædia Britannica (2008). "Ear, human," Encyclopædia Britannica 2006 Ultimate Reference Suite DVD, 22 Oct.
- Fay, R. R. (1988). *Hearing in Vertebrates: A Psychophysics Databook* (Hill-Fay Associates, Winnetka, IL).
- Felizardo, F. C., and Melville, W. K. (1995). "Correlations between ambient noise and the ocean surface wave field," *J. Phys. Oceanogr.* **25**, 515–532.
- Hornung, H. G., Willert, C., and Turner, S. (1995). "The flow field downstream of a hydraulic jump," *J. Fluid Mech.* **287**, 299–316.
- Koch, C., and Chanson, H. (2009). "Turbulence measurements in positive surges and bores," *J. Hydraul. Res.* **47**, 29–40.
- Kolaini, A. R., Roy, R. R., and Gardner, D. L. (1994). "Low-frequency acoustic emissions in fresh and salt water," *J. Acoust. Soc. Am.* **96**, 1766–1772.
- Larsonneur, C. (1989). "The bay of Mont-Saint-Michel: A sedimentation model in temperate environment," *Bull. Inst. Géol. Bassin d'Aquitaine, Bordeaux*, **46**, 5–73.
- Loewen, M. R., and Melville, W. K. (1991). "Microwave backscatter and acoustic radiation from breaking waves," *J. Fluid Mech.* **224**, 601–623.
- Manasseh, R., Bababin, A. V., Forbes, C., Rickards, K., Bobevski, I., and Ooi, A. (2006). "Passive acoustic determination of wave-breaking events and their severity across the spectrum," *J. Atmos. Ocean. Technol.* **23**, 599–618.
- Mason, T., Priestley, D., and Reeve, D. E. (2007). "Monitoring near-shore shingle transport under waves using a passive acoustic technique," *J. Acoust. Soc. Am.* **122**, 737–746.
- Melville, W. K., and Rapp, R. F. (1985). "Momentum flux in breaking waves," *Nature (London)* **317**, 514–516.
- Molchan-Douthit, M. (1998). *Alaska Bore Tales* (National Oceanic and Atmospheric Administration, Anchorage, AL).
- Monahan, G. (1981). "The tidal bore of the Maccan river," Musical piece.
- Moore, R. N. (1888). "Report on the Bore of the Tsien-Tang Kiang," Hydrographic Office, London.
- Nicholas, M., Roy, A. A., Crumb, L. A., Oguz, H., and Prosperetti, A. (1994). "Sound emissions by a laboratory bubble cloud," *J. Acoust. Soc. Am.* **95**, 3171–3182.
- Oguz, H. N., and Prosperetti, A. (1995). "Air entrapment by a falling water mass," *J. Fluid Mech.* **294**, 181–207.
- Prosperetti, A. (1988). "Bubble-related ambient noise in the ocean," *J. Acoust. Soc. Am.* **84**, 1042–1054.
- Tessier, B., and Terwindt, J. H. J. (1994). "An example of soft-sediment deformations in an intertidal environment—The effect of a tidal bore," *C. R. Acad. Sci., Ser. II.*, **319**, 217–233.
- Thorne, P. D. (1986). "Laboratory and marine measurements on the acoustic detection of sediment transport," *J. Acoust. Soc. Am.* **80**, 899–910.
- Wallace, D. W. R., and Wirick, C. D. (1992). "Large air-sea gas fluxes associated with breaking waves," *Nature (London)*, **356**, 694–696.
- Warfield, D. (1973). in *Methods of Animal Experimentation*, edited by E. Gay (Academic, London), Vol. **IV**, pp. 43–143.